Cl^- uptake promoting depolarizing GABA actions in immature rat neocortical neurones is mediated by NKCC1

Junko Yamada[1], Akihito Okabe[2], Hiroki Toyoda[2], Werner Kilb[3], Heiko J. Luhmann[3] and Atsuo Fukuda[1,2]

[1] *Department of Biological Information Processing, Graduate School of Electronic Science and Technology, Shizuoka University, Hamamatsu, Shizuoka 432-8011, Japan*

[2] *Department of Physiology, Hamamatsu University School of Medicine, Hamamatsu, Shizuoka 431-3192, Japan*

[3] *Institute of Physiology and Pathophysiology, Johannes Gutenberg-University, D-55099 Mainz, Germany*

GABA is the principal inhibitory neurotransmitter in the mature brain, but during early postnatal development the elevated $[Cl^-]_i$ in immature neocortical neurones causes $GABA_A$ receptor activation to be depolarizing. The molecular mechanisms underlying this intracellular Cl^- accumulation remain controversial. Therefore, the GABA reversal potential (E_{GABA}) or $[Cl^-]_i$ in early postnatal rat neocortical neurones was measured by the gramicidin-perforated patch-clamp method, and the relative expression levels of the cation−Cl^- cotransporter mRNAs (in the same cells) were examined by semiquantitative single-cell multiplex RT-PCR to look for statistical correlations with $[Cl^-]_i$. The mRNA expression levels were positively (the Cl^- accumulating Na^+,K^+−2Cl^- cotransporter NKCC1) or negatively (the Cl^- extruding K^+−Cl^- cotransporter KCC2) correlated with $[Cl^-]_i$. NKCC1 mRNA expression was high in early postnatal days, but decreased during postnatal development, whereas KCC2 mRNA expression displayed the opposite pattern. $[Cl^-]_i$ and NKCC1 mRNA expression were each higher in cortical plate (CP) neurones than in the presumably older layer V/VI pyramidal neurones in a given slice. The pharmacological effects of bumetanide on E_{GABA} were consistent with the different expression levels of NKCC1 mRNA. These data suggest that NKCC1 may play a pivotal role in the generation of GABA-mediated depolarization in immature CP cells, while KCC2 promotes the later maturation of GABAergic inhibition in the rat neocortex.

(Received 7 February 2004; accepted after revision 13 April 2004; first published online 16 April 2004)

Corresponding author J. Yamada: Department of Biological Information Processing, Graduate School of Electronic Science and Technology, Shizuoka University, Hamamatsu, Shizuoka 432-8011, Japan.
Email: djyamad@ipc.shizuoka.ac.jp

In immature neurones, GABA (γ-aminobutyric acid)$_A$ receptor-mediated responses are often depolarizing (Ben-Ari *et al.* 1989; Luhmann & Prince, 1991; LoTurco *et al.* 1995), which can trigger a number of developmental phenomena, e.g. neuronal proliferation, migration, and synaptogenesis (LoTurco *et al.* 1995; Behar *et al.* 1996; Ben-Ari, 2002). Thereafter, such depolarizing GABA actions shift to more negative levels during development. The accumulated evidence demonstrates that this GABA-induced membrane depolarization is caused by Cl^- efflux due to the high intracellular Cl^- concentration ($[Cl^-]_i$) maintained in immature cells (the direction of Cl^- currents being determined by $[Cl^-]_i$ and resting membrane potential) (Owens *et al.* 1996; for review, see Ben-Ari, 2002; Owens & Kriegstein, 2002; Payne *et al.* 2003).

Neuronal Cl^- homeostasis is maintained by the functional expression of Cl^- transporters and Cl^- channels. The Cl^--extruding KCC2 is generally considered to be involved in generating the hyperpolarizing effects of GABA, and a developmental up-regulation of KCC2 expression may underlie the GABAergic functional switch from excitatory to inhibitory (Rivera *et al.* 1999; DeFazio *et al.* 2000). In contrast, NKCC1 accumulates Cl^- into the cell under physiological conditions (Plotkin *et al.* 1997; Delpire *et al.* 1999; Sun & Murali, 1999). It may therefore contribute to the high $[Cl^-]_i$ found in immature neurones (Plotkin *et al.* 1997; Delpire *et al.* 1999; Shimizu-Okabe *et al.* 2002). However, because of a lack of direct evidence this role of NKCC1 remains controversial (Jarolimek *et al.* 1999; DeFazio *et al.* 2000; Balakrishnan *et al.* 2003).

J. Yamada and A. Okabe contributed equally to this work.

DOI: 10.1113/jphysiol.2004.062471

Although previous *in situ* hybridization and immunocytochemical studies have shown that NKCC1 mRNA and protein are abundant in neurones in the immature rat neocortex (Plotkin *et al.* 1997; Li *et al.* 2002; Shimizu-Okabe *et al.* 2002), evidence for a direct correlation with $[Cl^-]_i$ has not been obtained. For this purpose, measurement of $[Cl^-]_i$ and the identification of Cl^- transporter molecules in single neocortical cells is needed. In the present study, we measured GABAergic actions and $[Cl^-]_i$ by the gramicidin-perforated patch-clamp method, and examined the relative expression levels of Cl^- cotransporter mRNAs by semiquantitative single-cell multiplex RT-PCR. Our results strongly suggest that the high $[Cl^-]_i$ in immature neocortical neurones is maintained primarily by the presence of a differential expression of NKCC1 (relatively high) and KCC2 (relatively low). A subsequent up-regulation of KCC2 and down-regulation of NKCC1 causes a developmental decrease in $[Cl^-]_i$. As a result, $GABA_A$ receptor-mediated responses are transformed from depolarizing to hyperpolarizing in neocortical neurones. Some of the results have already been published in abstract form (Yamada *et al.* 2002).

Methods

All experiments conformed to the guidelines issued by Shizuoka University and Hamamatsu University School of Medicine on the ethical use of animals for experimentation, and all efforts were made to minimize the number of animals used and their suffering.

Brain slice preparation

The procedures used for preparing rat brain slices containing the neocortex were similar to those previously described (Toyoda *et al.* 2003). After the animals (63 Wister rats of postnatal day (P) 1–21) had been deeply anaesthetized by inhalation of halothane, they were decapitated; blocks of brain were quickly removed and placed in cold (4°C), oxygenated, modified artificial cerebrospinal fluid (ACSF). The solution contained the following (mM): 220 sucrose, 2.5 KCl, 1.25 NaH_2PO_4, 12.0 $MgSO_4$, 0.5 $CaCl_2{\cdot}2H_2O$, 26.0 $NaHCO_3$, 30.0 glucose (330–340 mosmol l^{-1}). Coronal slices (400 μm) of neocortex were cut in the modified ACSF using a vibratome (VT-100; Leica, Germany). Slices were allowed to recover for 60 min on nylon meshes (with 1 mm pores) placed on dishes and submerged in standard ACSF consisting of (mM): 126 NaCl, 2.5 KCl, 1.25 NaH_2PO_4, 2.0 $MgSO_4$, 2.0 $CaCl_2$, 26.0 $NaHCO_3$ and 20.0 glucose (310–315 mosmol l^{-1}). The dishes were placed in a tightly sealed box filled with 95% O_2–5% CO_2 at a pressure of 50 kPa at room temperature.

Gramicidin-perforated patch-clamp recordings

The slices were transferred to a recording chamber on the stage of a microscope (BH2; Olympus, Japan) and continuously perfused with oxygenated, standard ACSF at a flow rate of 2 ml min^{-1} and a temperature of 30°C. During voltage-clamp recording, 0.5 μM tetrodotoxin (TTX) was present to block Na^+-dependent action potentials, and CGP55845 to antagonize $GABA_B$ receptors. Gramicidin-perforated patch-clamp recording (Ebihara *et al.* 1995) was performed as previously described (Toyoda *et al.* 2003). Neocortical neurones in the slices were viewed on a monitor via a 40 × water-immersion objective lens with an infrared differential interference contrast (IR-DIC) filter, and a CCD-camera (C2400-79H; Hamamatsu Photonics, Japan). Real-time video images were contrast-enhanced by a video processor (Argus-20; Hamamatsu Photonics, Japan).

Patch electrodes were fabricated from borosilicate capillary tubing of 1.5 mm diameter (Garner Glass Company, USA) using a Narishige PP-83 vertical puller (Narishige, Japan). The electrode resistance ranged from 3 to 4.5 MΩ. The pipette solution contained (mM): 150 KCl and 10 Hepes (pH 7.3 with KOH). Gramicidin was dissolved in dimethylsulfoxide (10 mg ml^{-1}), then diluted in the pipette-filling solution to a final concentration of 5–10 μg ml^{-1} just before the experiment. Membrane currents and membrane potentials were recorded using an Axopatch 1D amplifier and digitized at 5–10 kHz by means of a Digidata 1332A data-acquisition system (Axon Instruments, USA). Data were acquired by means of pCLAMP8 (Axon Instruments) software and stored on the hard disk for off-line analysis using Clampfit8 (Axon Instruments). Series resistance, R_s, compensation was not applied. To measure the reversal potential for the GABA-induced current (E_{GABA}), voltage steps were applied, and at each membrane potential GABA (50 μM) was pressure-applied for 10–50 ms through a patch pipette to the soma of the recorded neurones. Peak current responses for each voltage were plotted, and the data were fitted using KyPlot software (Kyence Inc., Japan).

Intracellular chloride estimation

Cells were voltage-clamped at −60 mV and stepped to various test potentials. The series resistance (estimated from the peak transient during the 10 mV test pulse delivered before each trial) and the amplitude of the

current (before baseline correction) at 100–200 ms from the time of the pressure application were used to calculate the voltage error caused by uncorrected series resistance. The baseline current (determined at 20 ms before the start of the pressure pulse) was subtracted from the absolute current amplitude (baseline-corrected traces). To obtain *I–V* curves from gramicidin recordings, the membrane potential values were corrected for the voltage drop across the series resistance: $V_{corr} = V_{com} - I_{clamp} \times R_s$, where V_{com} is the command potential, I_{clamp} is the clamp current (50–100 pA), and R_s is the series resistance (<40 MΩ). These values were plotted as a function of the series resistance-corrected membrane potential. The $[Cl^-]_i$ was calculated from the reversal potential of the GABA-evoked currents according to the Nernst equation.

Semi-quantitative single-cell multiplex RT-PCR analysis

To harvest cytoplasm for the subsequent single-cell RT-PCR reaction, each patch-clamp pipette was filled with 10 μl gramicidin-containing pipette solution. After patch-clamp recording, mild suction was used to aspirate the contents of the cell into the tip of the recording electrode, and this was then expelled into a microfuge tube. Subsequently, harvested cytoplasm was frozen with crushed dry ice, and stored at −80°C for at most 2 days. Several target sequences were simultaneously amplified from a single cDNA synthesis by multiplex PCR using nested primers and two rounds of amplification. RT and first-round PCR reactions were performed in the same tube using a OneStep RT-PCR kit (Qiagen, GmbH, Germany). The thin-walled PCR tube contained 10 μl solution with cytoplasm, 5 × Qiagen OneStep RT-PCR buffer (10 μl), Qiagen OneStep RT-PCR enzyme mix (2 μl), 0.4 mM of each dNTP, 8 units of RNase inhibitor (Promega, Tokyo, Japan), and 0.6 μM of each outside primer in a buffer supplied by the manufacturer (reaction volume, 50 μl). After the RT reaction had proceeded at 50°C for 30 min, first-round PCR was subsequently performed in the same tube with a 15-min pre-incubation at 95°C followed by 40 cycles (each of 30 s at 94°C (denaturation), 30 s at 55°C (annealing), and 1 min at 72°C (extension)) in a thermal cycler (PC-801; ASTEC Co. Ltd, Fukuoka, Japan). Subsequently, first-round PCR products were diluted 1000-fold, and the amplification involved a hot start at 95°C for 15 min, denaturation at 94°C for 30 s, annealing at 60°C for 30 s, and extension at 72°C for 1 min in separate reactions using the internal primer pairs for each template. The second-round PCR reaction was performed using 10 × PCR buffer (5 μl), 3 mM $MgCl_2$, 0.2 mM of each dNTP (Amersham Bioscience, Tokyo, Japan), and 1.25 units HotStarTaq DNA polymerase (Qiagen, GmbH) in the supplied buffer plus enzyme (reaction volume, 50 μl). To ensure that saturation did not occur during PCR, a kinetic analysis was performed using multiple aliquots for each cell to verify that all readings were taken in the exponential phase of amplification. A cycle number at which all cells were in the exponential phase was selected (β-actin, 11 cycle; KCC2, 18 cycle; NKCC1, 26 cycle), and for each mRNA species the PCR products from the selected cycle were analysed together for all cells.

PCR fragments were gel-purified and confirmed by DNA sequencing. The PCR products of the aliquots were analysed by 10% acrylamide gel electrophoresis, and quantified using SYBR green I (Molecular Probes, Inc., Eugene, OR, USA). Bands were analysed on an imaging plate (EDAS 290; Kodak, NY, USA) with the aid of KODAK 1D software (Eastman Kodak). In all these semiquantitative comparisons, the optical densities of the KCC2 and NKCC1 bands were expressed relative to the optical density of the internal standard represented by the β-actin product band under the same contrast conditions (Brooks-Kayal *et al.* 1998).

Nested PCR primers

The nested primers used for the PCR analyses were selected on the basis of known rat cDNA or genomic sequences, and are given here (the outside primer pair is listed first in each case; the size of the final amplification product, shown in parenthesis, is not the final size, but the size of the region of the gene used as primer): β-actin (GenBank no. V01217 Nudel *et al.* 1983), 5′-ACACGGCATTGTAACCAACT-3′/5′-CATTGCCGATAGTGATGACC-3′ and 5′-AGAAGATTTGGCACCACACT-3′/5′-CCATCTCTTGCTCGAAGTCT-3′ (1578–2476 nt); KCC2 (GenBank no. U55816 Gillen *et al.* 1996), 5′-GATGAAGAAAGACCTGACCA-3′/5′-CTGGTTCAAGTTTTCCCACT-3′ and 5′-CATTCGGAGGAAGAATCCAG-3′/5′-TTTGTTCTTCTGAGCCGCTG-3′ (2935–3172 nt); NKCC1 (GenBank no. AF051561 Moor-Hoon & Turner, 1998), 5′-GAAAGTACTCCAACCAGAGA-3′/5′-AGCTAGAATACCAGTTGCAG-3′ and 5′-TTGTCATGGATTGTGGGTCA-3′/5′-GAATCACCAGAAGGACGATC-3′ (1022–1424 nt).

Ca^{2+} imaging using fura-2

The methods used for Ca^{2+} imaging in brain slices were similar to those previously described (Toyoda *et al.* 2003).

Neurones were loaded with the Ca^{2+} indicator fura-2 by incubating slices for 90 min with fura-2 acetoxylmethyl ester (10 μM) in ACSF containing 0.01% pluronic F127 under the conditions described for recovery of slices, followed by washing with standard ACSF. Slices, which were then laid on the glass bottom of a submerged-type chamber placed on a microscope stage, were continuously perfused at a rate of 2–3 ml min^{-1} with standard ACSF gassed with 95% O_2–5% CO_2. The bathing solution, which was maintained at a temperature of 30°C, had a pH of 7.4. Fura-2 fluorescence was excited by means of a multiwavelength monochrometer (C6789; Hamamatsu Photonics, Japan), and the emitted light was filtered through a band-pass filter (510 nm). Fluorescence images were obtained using a 40 × objective lens (Plan Fluor, N.A. 0.75; Nikon, Japan) via a cooled-CCD camera (C6790; Hamamatsu Photonics, Japan) fitted to an upright microscope (E600-FN; Nikon, Japan). Data were stored for off-line analysis using image-processing software (Aquacosmos; Hamamatsu Photonics, Japan). $[Ca^{2+}]_i$ was expressed as the ratio of the fura-2 fluorescence intensity excited at 340 nm over that excited at 380 nm ($R_{F_{340}/F_{380}}$). The $R_{F_{340}/F_{380}}$ value was monitored in neurones and measurements were taken every 10 s. Drugs were applied by bath perfusion in the Ca^{2+}-imaging experiments.

Drugs

The following drugs were used: fura-2 acetoxylmethyl ester, dimethylsulfoxide (−)-bicuculline methiodide, *R*(+)-[(2-*n*-butyl-6,7-dichloro-2-cyclopentyl-2,3-dihydro-1-oxo-1-H-indenyl-5-yl)-oxy] acetic acid (DIOA), GABA, L-glutamate, gramicidin D, nifedipine, and picrotoxin (Sigma), bumetanide and CGP55845 (Tocris), and TTX (Wako).

Statistics

Numerical data are presented as means ± S.D. Unless otherwise noted, statistical significance was determined using a two-tailed Student's *t* test at the $P < 0.05$ level.

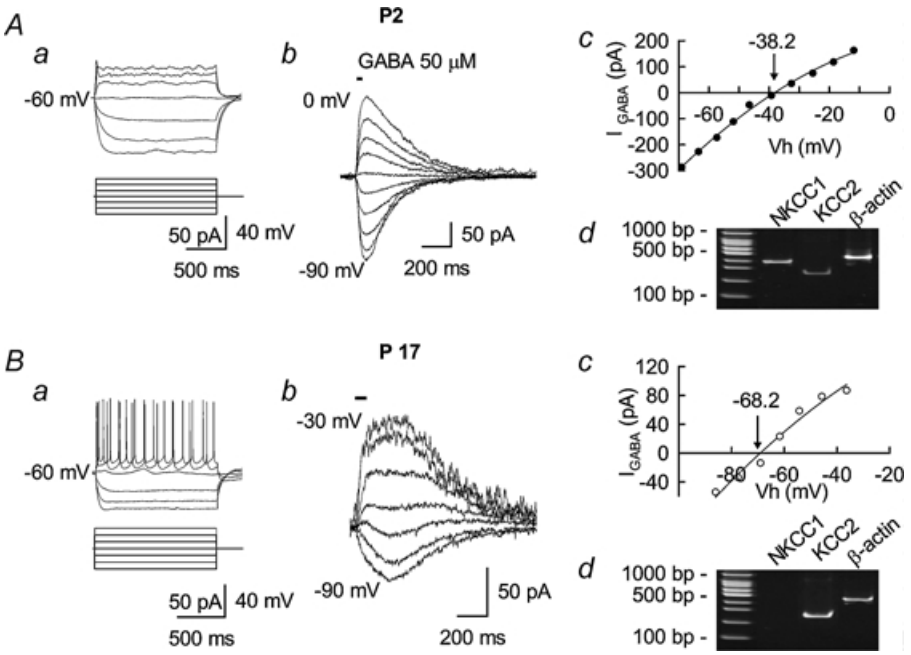

Figure 1. Typical gramicidin-perforated patch-clamp recordings, with subsequent single-cell multiplex RT-PCR, in cortical plate (CP) and layer II/III pyramidal neurones

A, CP neurone at P2. *B*, layer II/III pyramidal neurone at P17. *a*, voltage responses to current injections recorded in current-clamp mode reveal strong adaptation of action potentials in P2 (*Aa*), but not in P17 (*Ba*) neurones. *b*, GABA (50 μM)-induced currents at different command potentials reveal more negative reversal potential at P17 (*Bb*) than at P2 (*Ab*). *c*, current–voltage relationship estimated from the peak current measured during the responses shown in *b* shows that the E_{GABA} values determined by fitting the *I–V* curve to a second-order polynomial function were −38.2 mV at P2 (*Ac*) and −68.2 mV at P17 (*Bc*). *d*, single-cell mRNA expression profiles for NKCC1, KCC2 and β-actin. Note that the P17 cell was lacking in NKCC1 (*Bd*), while the P2 cell had a weaker expression of KCC2 (*Ad*) than the P17 cell (*Bd*). All P2 data (*A*) were obtained from the same cell, as were the P17 data (*B*).

Results

Membrane properties and GABA actions in developing neocortical cells

Neocortical neurones were identified using IR-DIC video microscopy by the shape of their soma. These cells were classified either as CP cells or as layer II/III or layer V/VI pyramidal cells according to their age and location within the somatosensory cortex. Immature P1–3 neocortical cells comprised small, non-ramified neurones located within or beneath the CP, and these were termed CP cells. They had a large input resistance ($1588 \pm 480\ M\Omega$) and their average resting membrane potential was -50.7 ± 4.7 mV ($n = 15$), values consistent with those previously reported (Luhmann *et al.* 1999). In contrast, P11–20 layer II/III more mature pyramidal neurones had a larger, pyramidal-shaped soma and a lower input resistance ($430 \pm 111\ M\Omega$) than P1–3 cells, and their resting membrane potential was -64.0 ± 3.6 mV ($n = 10$). Suprathreshold depolarization elicited only one action potential in all CP neurones tested at P1–3 (Fig. 1*Aa*). In contrast, P11–20 layer II/III pyramidal neurones generated trains of action potentials upon depolarizing-current injections (Fig. 1*Ba*).

Gramicidin-perforated patch-clamp recordings were performed to quantify the developmental changes in GABA responses. Reversal potentials were determined for GABA-evoked currents (E_{GABA}) by applying GABA to the cells being recorded while voltages were clamped at different holding potentials. Examples for individual cells are shown in Fig. 1, and group data in Fig. 2.

Developmental negative shift in E_{GABA}, and changes in NKCC1 and KCC2 mRNA expressions

To test whether a developmental shift in E_{GABA} or decrease in $[Cl^-]_i$ occurs and whether it is regulated by KCC2 and NKCC1 expressions, the mRNAs for these transporters were studied by applying multiplex RT-PCR to cells in which $[Cl^-]_i$ had been estimated from the E_{GABA} value (Figs 1 and 2). The mean E_{GABA} was significantly more positive in immature CP cells (-40.5 ± 2.4 mV, $n = 15$) than in mature layer II/III neurones (-71.5 ± 2.1 mV, $n = 10$) (Fig. 2*A*). NKCC1 mRNA expression was not detected by our single-cell RT-PCR in any of the more mature neurones recorded (Fig. 2*B*), although it was observed to some extent by using other methods (Sun & Murali, 1999; Shimizu *et al.* 2002).

The $[Cl^-]_i$ calculated from E_{GABA} was significantly larger in P1–3 CP neurones (29.5 ± 8.8 mM; $n = 15$) than in P11–20 layer II/III neurones (8.6 ± 2.1 mM; $n = 10$) (Fig. 3*A*). Application of single-cell multiplex RT-PCR to these developing neurones (from P1–3 to P11–20) revealed that the developmental decline in $[Cl^-]_i$ was accompanied by a significant up-regulation of KCC2 mRNA (Fig. 3*B*) and a disappearance of NKCC1 mRNA (Fig. 3*C*). To compare the expression level of each Cl^- transporter mRNA among cells, NKCC1 and KCC2 signal intensities were normalized with respect to that of β-actin.

$[Cl^-]_i$ and Cl^- transporter mRNA expressions in relation to neuronal birth date

The six neocortical layers are formed during development as neurones migrate toward the pial surface and come to

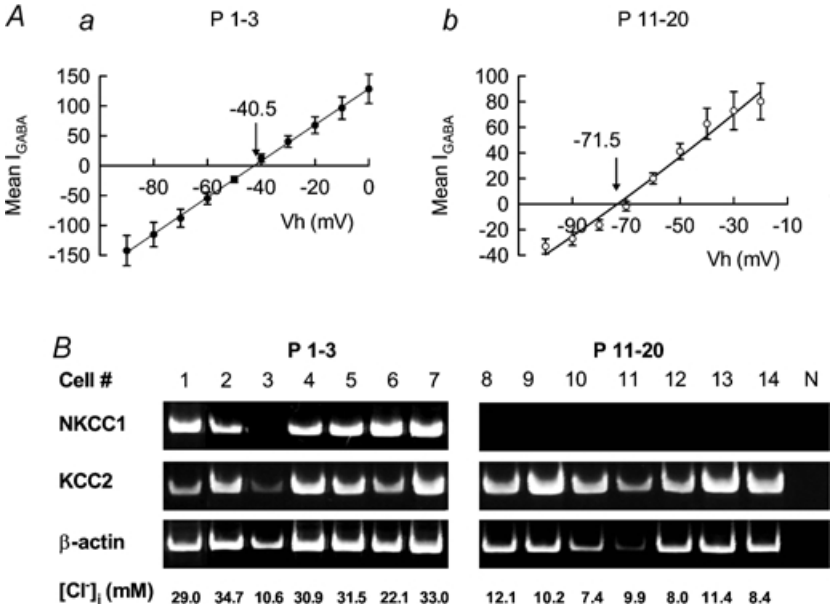

Figure 2. Negative shift in E_{GABA} during development
A, averaged GABA-induced current plotted as a function of membrane potential (*I–V* relationship) for P1–3 (*a*, $n = 15$) and P11–20 (*b*, $n = 10$) neurones. E_{GABA} was significantly more positive at P1–3 than at P11–20. Error bars indicate S.E.M. *B*, expressions of NKCC1, KCC2 and β-actin mRNAs were detected by means of single-cell multiplex RT-PCR from the cells used for *A*. N: negative control using RNase- and DNase-free water. Note that NKCC1 mRNA was not detected at all in P11–20 cells.

occupy their final positions, with the neurones of layers II–VI being arranged eventually in an inside-out manner (those in the deepest layer, layer VI, having been born first, at E12–15 (Valverde *et al.* 1989), and those in layer II last, at E17–P1 (Hicks & D'Amato, 1968)). Thus, on early postnatal days the (younger) CP neurones might be expected to have a higher $[Cl^-]_i$ than the (older) layer V/VI neurones in a given animal. As seen in one and the same slice, CP contained neurones with a small-sized soma and without apparent apical dendrites, whereas layer V/VI contained neurones with a large, pyramidal-shaped soma and apical dendrites (Fig. 4*Aa* and *Ab*). At P1–3, the E_{GABA} was more positive in CP cells than in layer V/VI neurones, and hence $[Cl^-]_i$ was significantly lower in the latter than in the former. At P5–7, $[Cl^-]_i$ showed a negative shift *versus* P1–3 in both layer II/III and layer V/VI neurones (Fig. 4*C*). At P1–3, but not at P5–7, the expression level for NKCC1 mRNA was significantly higher in CP neurones than in layer V/VI neurones (Fig. 4*D*). However, no such difference was observed in the expression level of KCC2 (Fig. 4*E*), indicating that NKCC1 plays an essential role in generating the higher $[Cl^-]_i$ in CP cells.

Differential effect of Cl^- transporter inhibitors on E_{GABA} in immature and mature neurones

In the presence of bumetanide, a specific inhibitor of the Na^+,K^+−2 Cl^- cotransporter, immature neurones (Fig. 5*Aa*), but not mature neurones (Fig. 5*Ba*), displayed a negative shift in E_{GABA}. In line with this pharmacological effect, NKCC1 mRNA was found to be expressed in the bumetanide-sensitive neurones (Fig. 5*Ab*), but not in the bumetanide-insensitive ones (Fig. 5*Bb*). The E_{GABA} value obtained for the NKCC1-expressing cells (-39.2 ± 5.9 mV, $n = 5$) was significantly more positive than that obtained for the NKCC1-negative cells (-64.8 ± 12.1 mV, $n = 4$) (Fig. 5*C*). The shift in E_{GABA} induced by bumetanide was significantly greater in the NKCC1-expressing cells than in the NKCC1-negative neurones (Fig. 5*D*).

In immature cells, E_{GABA} was not changed significantly in the presence of DIOA, an inhibitor of the K^+–Cl^- cotransporter (Fig. 6*A*). In contrast, in mature cells DIOA reversibly shifted E_{GABA} in the positive direction (Fig. 6*B*). The E_{GABA} of the DIOA-sensitive neurones was significantly more negative than that of the DIOA-insensitive ones (Fig. 6*C*). The DIOA-induced positive shift in E_{GABA} tended to become greater as the KCC2 expression level increased, although a significant correlation was not established (Fig. 6*D*).

Positive and negative correlations of NKCC1 and KCC2 mRNA expression levels, respectively, with $[Cl^-]_i$

In 42 cells in which $[Cl^-]_i$ was measured using the gramicidin-perforated patch-clamp method, single-cell multiplex RT-PCR was performed to compare the relative expression levels of NKCC1 and KCC2 mRNAs among cells. Then, the normalized NKCC1 and KCC2 mRNA levels in individual cells were statistically analysed for their correlation with $[Cl^-]_i$. Using multiple regression analysis, we found that $[Cl^-]_i$ displayed a positive correlation

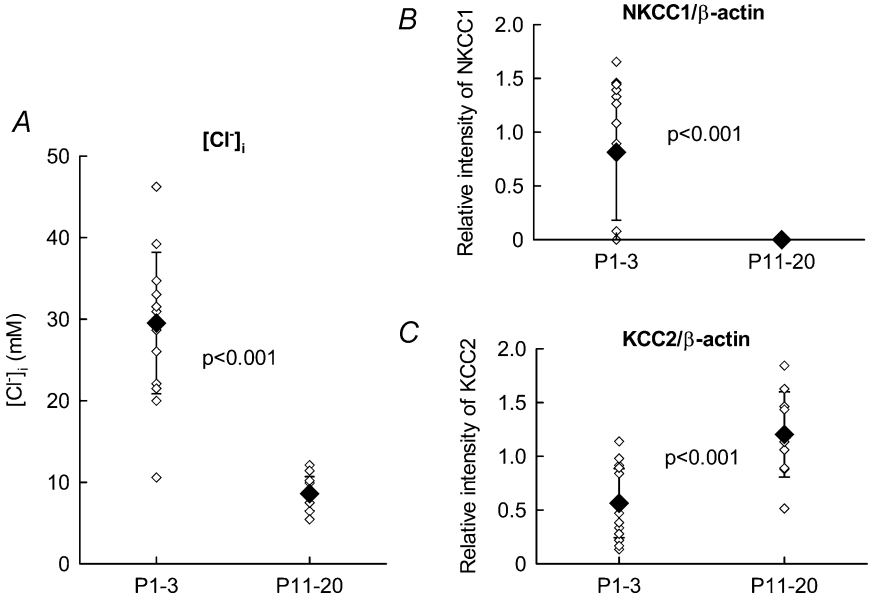

Figure 3. Changes in $[Cl^-]_i$ and expression levels of NKCC1 and KCC2 mRNAs during development
A, the calculated $[Cl^-]_i$ values were plotted for P1–3 ($n = 15$) P11–20 neurones ($n = 10$) (◆ : mean ± S.D.). The expression levels of NKCC1 and KCC2 mRNAs (harvested from the same cells as in *A*) are shown in *B* and *C*, respectively. The intensity of the PCR products for NKCC1 and KCC2 mRNAs were normalized with respect to that for *β*-actin. The relative intensity for NKCC1 mRNA decreased significantly, from 0.8 ± 0.6 to 0, whereas that for KCC2 mRNA increased significantly, from 0.6 ± 0.3 to 1.2 ± 0.4.

with NKCC1 mRNA ($r_{NKCC1,[Cl]_i} = 0.65$, partial correlation coefficient; $P < 0.001$), but a negative correlation with KCC2 mRNA ($r_{KCC2,[Cl]_i} = -0.32$; $P < 0.05$) (Fig. 7). This suggests that NKCC1 accumulates Cl^- into the cell, while KCC2 extrudes it out of the cell.

$GABA_A$ receptor-mediated Ca^{2+} transients in developing cortical neurones

Application of GABA (10 μM) evoked transient increases in $[Ca^{2+}]_i$ in CP neurones. These transients were abolished both by the $GABA_A$ receptor antagonist picrotoxin (50 μM) ($n = 58$; 3 slices) and by the L-type Ca^{2+} channel blocker nifedipine (100 μM) ($n = 53$; 3 slices), but not by TTX (3 μM) ($n = 53$; 3 slices) (Fig. 8*A*). Bumetanide (20 μM) ($n = 38$; 3 slices) also abolished the GABA-evoked $[Ca^{2+}]_i$ increases, but DIOA did not ($n = 43$; 3 slices).

When the GABA-induced Ca^{2+} transient was compared to that induced by glutamate at the same concentration (10 μM), brief application of GABA was found to evoke a significantly greater increase in $[Ca^{2+}]_i$ than glutamate (Fig. 8*B*) ($n = 53$; 3 slices). When the GABA-induced Ca^{2+} transients were compared between the superficial layer (CP or layer II/III) and layer V/VI, those in the former were significantly larger than those in the latter at P0, P2 and P4. The difference gradually declined as development proceeded, and no significant difference was observed between superficial and layer V/VI neurones at P6 ($n = 46-61$ for CP, $n = 46-62$ for layer V/VI; 3 slices at each age) (Fig. 8*C*).

Discussion

Candidates for the regulator of the depolarizing actions of GABA and the associated Ca^{2+} influx

$GABA_A$ receptor activation leads to depolarization and a $[Ca^{2+}]_i$ transient in immature neurones in a number of brain regions including the neocortex (Connor *et al.* 1987; Ben-Ari *et al.* 1989; Cherubini *et al.* 1990; Luhmann & Prince, 1991; Yuste & Katz, 1991; Leinekugel *et al.* 1995; Owens *et al.* 1996). In the present study, CP neurones were found to have an E_{GABA} positive to the resting membrane potential, so that GABA depolarized the membrane potential and induced a marked rise in intracellular Ca^{2+}. These Ca^{2+} transients were reversibly abolished by picrotoxin and by nifedipine, but not by TTX, indicating that the $GABA_A$ receptor-mediated depolarization exceeds

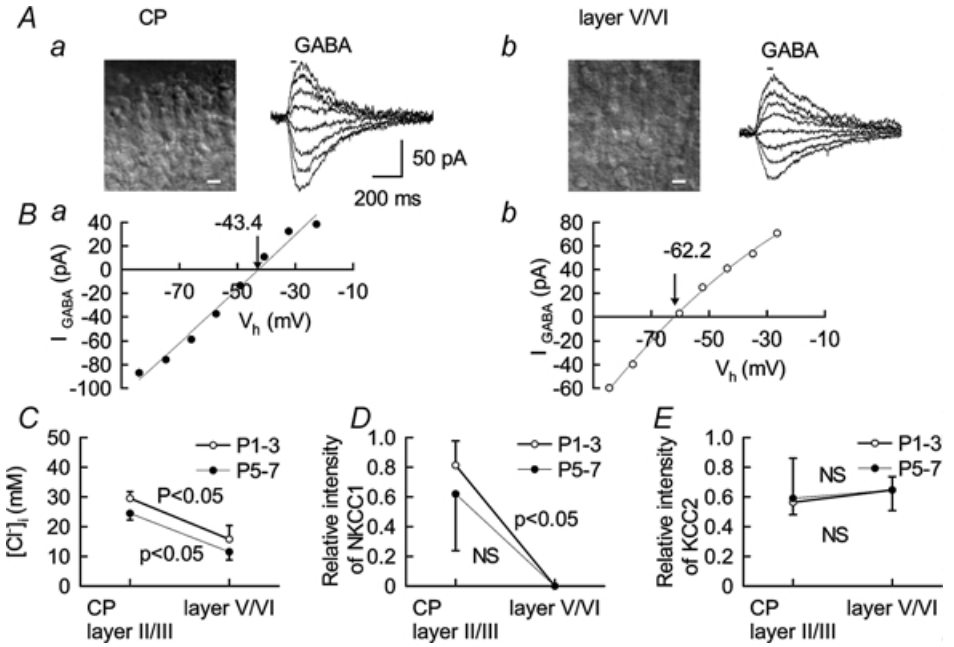

Figure 4. Regional differences in $[Cl^-]_i$ and Cl^- transporter mRNA expression in the same slice
A, IR-DIC images and GABA-evoked currents for cells in CP (*a*) and layer V/VI (*b*) of a P4 rat. *B*, current–voltage relationships for the GABA-induced currents in the CP (*a*) and layer V/VI (*b*) neurones shown in *Aa* and *Ab*. *C*, $[Cl^-]_i$ was significantly higher in CP cells than in layer V/VI neurones at either P1–3 ($n = 15$ and 4, respectively) or P5–7 ($n = 5$ and 5, respectively). *D*, normalized NKCC1 mRNA expression (as estimated by single-cell RT-PCR) was significantly higher in CP than in layer V/VI neurones (in the same slices) at P1–3, but not at P5-7. *E*, normalized KCC2 mRNA expression was not significantly different between CP and layer V/VI at either P1–3 or P5–7.

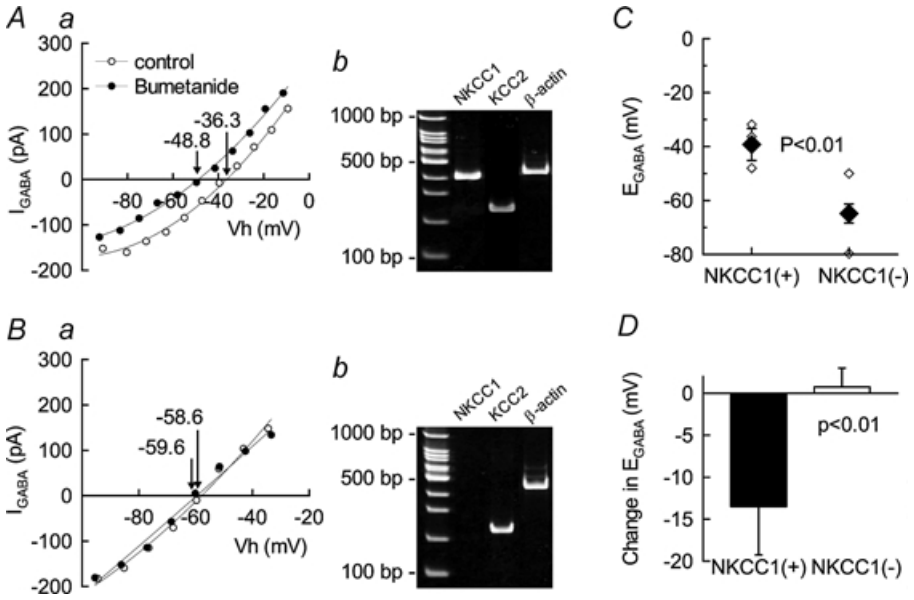

Figure 5. Differential effects of a Na^+,K^+–$2Cl^-$ cotransporter inhibitor on NKCC1-expressing and NKCC1-negative neurones

Bumetanide (20 μM) shifted E_{GABA} in the negative direction in NKCC1-expressing P2 CP neurones (*A*), but not in NKCC1-negative P5 layer V/VI neurones (*B*). The expression profiles of the NKCC1 and KCC2 mRNAs were confirmed by single-cell multiplex RT-PCR (*b*). *C*, E_{GABA} was significantly more positive in NKCC1-expressing (+) cells ($n = 5$) than in NKCC1-negative (−) cells ($n = 4$). *D*, the bumetanide-induced negative shift in E_{GABA} was significantly larger in NKCC1-expressing than in NKCC1-negative neurones.

the threshold for the voltage-dependent L-type Ca^{2+} channels irrespective of action potential firing.

In our study, the resting membrane potential was -50.7 ± 4.7 mV in P1–3 CP neurones, in accord with a previous report (Luhmann *et al.* 1999). Recently, Tyzio *et al.* (2003) have reported that the apparently depolarized membrane potential of immature neurones with a high resistance observed in perforated and whole-cell recordings is due to a shunt through the seal between the patch pipette and the membrane. According to their methods, the estimated resting membrane potential in the present study was −71.5 mV in P1–3 CP neurones.

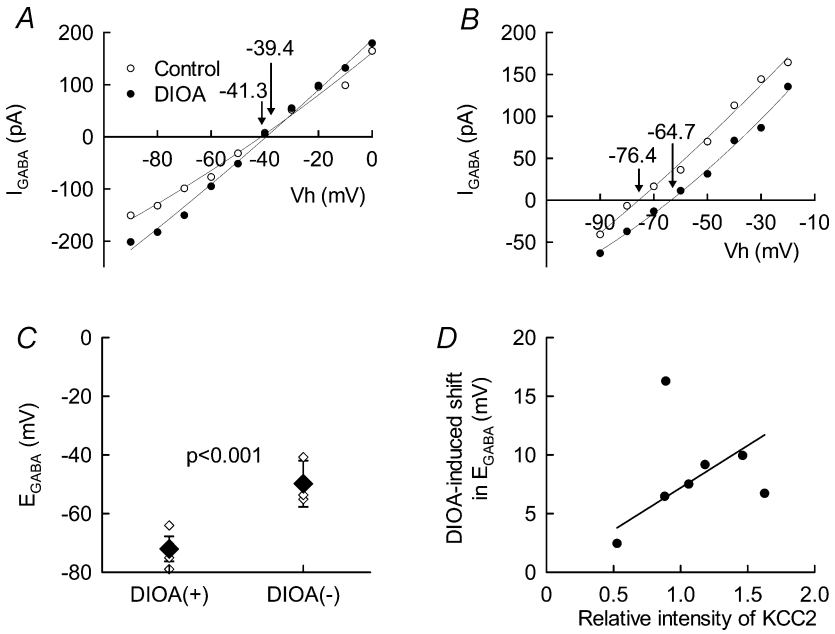

Figure 6. Differences in Cl^- homeostasis as a function of K^+–Cl^- cotransporter expression level

The K^+–Cl^- cotransporter inhibitor DIOA (50 μM) did not alter E_{GABA} in immature neurones (P3 CP, *A*), but it shifted E_{GABA} in the positive direction in mature neurones (P19 layer II/III, *B*). *C*, E_{GABA} was significantly more negative in DIOA-sensitive (+) neurones ($n = 6$) than in DIOA-insensitive (−) neurones ($n = 4$). *D*, plot of the effect of DIOA on E_{GABA} against the KCC2 mRNA expression level ($n = 7$). The line was fitted by eye.

Thus, in immature neurones GABA would cause a greater depolarization.

Accumulating evidence indicates a developmental shift in E_{GABA} from a level positive to the resting potential toward a more hyperpolarized potential, most likely the result of an ontogenic decrease in $[Cl^-]_i$ (Cherubini *et al.* 1990; Luhmann & Prince, 1991; Owens *et al.* 1996; Shimizu-Okabe *et al.* 2002). The K^+-Cl^- cotransporter KCC2 increases the rate of Cl^- extrusion, thus leading to a reduction in $[Cl^-]_i$ and a consequent negative shift in E_{GABA} (Payne, 1997; Jarolimek *et al.* 1999; Kakazu *et al.* 2000). Indeed, the change in the KCC2 mRNA level correlates with the ontogenic switch in GABAergic transmission from depolarization to hyperpolarization (Rivera *et al.* 1999). Moreover, KCC2 can move Cl^- into the cell when the extracellular K^+ increases (Jarolimek *et al.* 1999; Kakazu *et al.* 2000; DeFazio *et al.* 2000). Thus, it is well established that KCC2 is the key factor in a homeostatic switch in the way $[Cl^-]_i$ regulates the actions of GABA (for review, see Ben-Ari, 2002; Payne *et al.* 2003). However, the weak expression of KCC2 in immature neurones cannot by itself explain their E_{GABA} (or E_{Cl}) being positive to the resting membrane potential and rendering the action of GABA depolarizing.

Bicarbonate may also be an important component in the depolarizing GABA responses (Kaila & Voipio, 1987; Kaila *et al.* 1989; Staley *et al.* 1995); however, the bicarbonate contribution would be expected to be smaller in immature neurones (Owens *et al.* 1996; Kilb *et al.* 2002) than in adult neurones (Kaila *et al.* 1993). When considered for bicarbonate permeability (using the Goldman–Hodgkin–Katz equation with $[HCO_3^-]_o = 26$ mM, $[HCO_3^-]_i = 16$ mM (Dalwig *et al.* 1999) and $P_{HCO_3}/P_{Cl} = 0.2$ (Kaila *et al.* 1993), the $[Cl^-]_i$ values in more mature (P11–20) neurones became smaller, and the difference in $[Cl^-]_i$ between immature and more mature neurones was even greater (i.e. immature $\gg$mature). All this strongly suggests the existence of a Cl^- accumulating mechanism in immature neurones.

Ontogeny of Cl^- homeostasis is regulated not only by KCC2, but also by NKCC1

Here, we have characterized the electrophysiological (GABA responses) and molecular biological (mRNA expressions) characteristics of Cl^- transporters. However, we should make two provisos: (a) protein levels do not always relate to the mRNA expression levels (Sun & Murali, 1999; Shimizu-Okabe *et al.* 2002), and (b) the protein and activity levels might conceivably be regulated by some other factors (Kelsch *et al.* 2001). Nevertheless, our use of gramicidin-perforated patch-clamp recording, which does not alter $[Cl^-]_i$, followed by semiquantitative single-cell multiplex RT-PCR analysis in the same cells revealed that the expression levels of NKCC1 and KCC2 mRNAs correlated well with the electrophysiological evidence of $[Cl^-]_i$ changes.

Pharmacological inhibition of the Na^+,K^+-2Cl^- cotransporter by bumetanide application (Gillen *et al.*

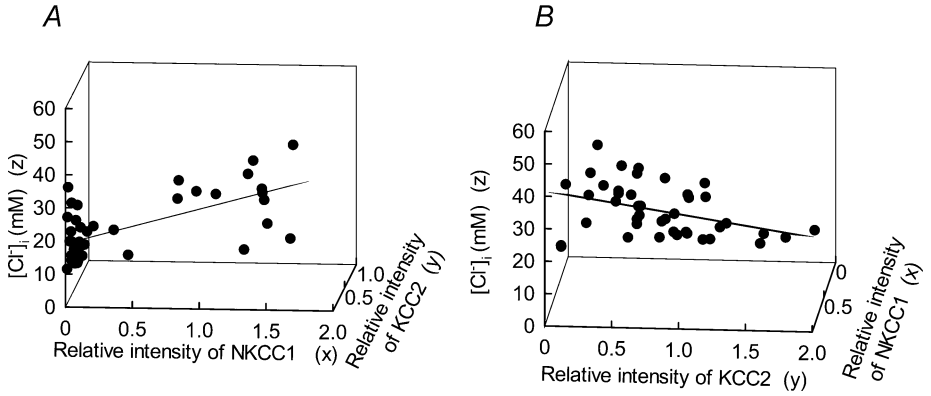

Figure 7. Correlation of expressions of NKCC1 and KCC2 mRNAs with $[Cl^-]_i$

$[Cl^-]_i$ is plotted against the relative expression levels of the mRNAs for both NKCC1 and KCC2 (normalized with respect to β-actin) in the same cell ($n = 42$). The bivariate linear regression was fitted to the data points by the least-squares method ($z = 19.2 + 10x - 6.2y$; where z is $[Cl^-]_I$, x is normalized expression level for NKCC1 mRNA, and y is normalized expression level for KCC2 mRNA). The above equation indicates that if neither NKCC1 nor KCC2 was operating, $[Cl^-]_i$ would be 19.2 mM ($E_{Cl} = -50.5$ mV). Note that the cubic graphs in *A* and *B* are identical ones viewed from different angles. *A*, in this view of the bivariate linear regression, the positive slope for x indicates a significant positive correlation between NKCC1 mRNA and $[Cl^-]_i$ ($r_{NKCC1,[Cl]_i} = 0.65$). *B*, in this view of the regression, the negative slope for y indicates a significant negative correlation between KCC2 mRNA and $[Cl^-]_i$ ($r_{KCC2,[Cl]_i} = -0.32$). Thus, NKCC1 and KCC2 had opposite correlations with $[Cl^-]_i$.

1996; Van Aubel *et al.* 2000; Payne *et al.* 2003) led to a negative shift in E_{GABA} in high-$[Cl^-]_i$ cells, in which NKCC1 mRNA was expressed, but had no effect on low-$[Cl^-]_i$ neurones, in which NKCC1 mRNA expression was not detected. Hence, at the single-cell level bumetanide's pharmacological effects correlated with the NKCC1 mRNA expression. These data suggest that NKCC1 is pivotal in determining the Cl^- concentration gradient across the membrane. This is in agreement with a previous finding of a significant reduction in basal Cl^- concentration in dorsal root ganglion neurones in the NKCC1 knock-out mouse (Sung *et al.* 2000). Although NKCC1 mRNA was not detected after P11 at single pyramidal cell level, the mRNA and protein expressions of NKCC1 could be observed by using *in situ* hybridization, immunostaining and immunoblotting methods (Clayton *et al.* 1998; Sun & Murali, 1999). This discrepancy might be due to different materials and methods used as discussed elsewhere (Shimizu-Okabe *et al.* 2002). In any case, the present results are consistent with our previous study (Shimizu-Okabe *et al.* 2002).

Although DIOA is reportedly selective for K^+-Cl^- cotransporters over Na^+,K^+-2Cl^- cotransporters (Garay *et al.* 1988), it also inhibits NKCC1 (Gillen *et al.* 1999). Thus, the effect of DIOA, like that of furosemide (Gillen *et al.* 1996; Payne *et al.* 2003), may not be so specific. Under our recording conditions, however, DIOA was effective only on neurones with an E_{GABA} negative to the resting membrane potential, and it was more effective on those cells with a relatively high KCC2 mRNA expression. Moreover, its effects were comparable to those induced by furosemide (not shown). Thus, the DIOA-sensitive K^+-Cl^- cotransporter responsible for Cl^- extrusion under our conditions could be KCC2 (Coull *et al.* 2003). Therefore, Cl^- accumulation in immature cells would not be mediated by KCC2, where DIOA and furosemide were ineffective.

Our results showed that E_{GABA} was significantly more positive in early postnatal CP cells than in mature neurones. Moreover, NKCC1 mRNA expression was significantly higher on early than on later postnatal days, and it decreased rapidly during postnatal development.

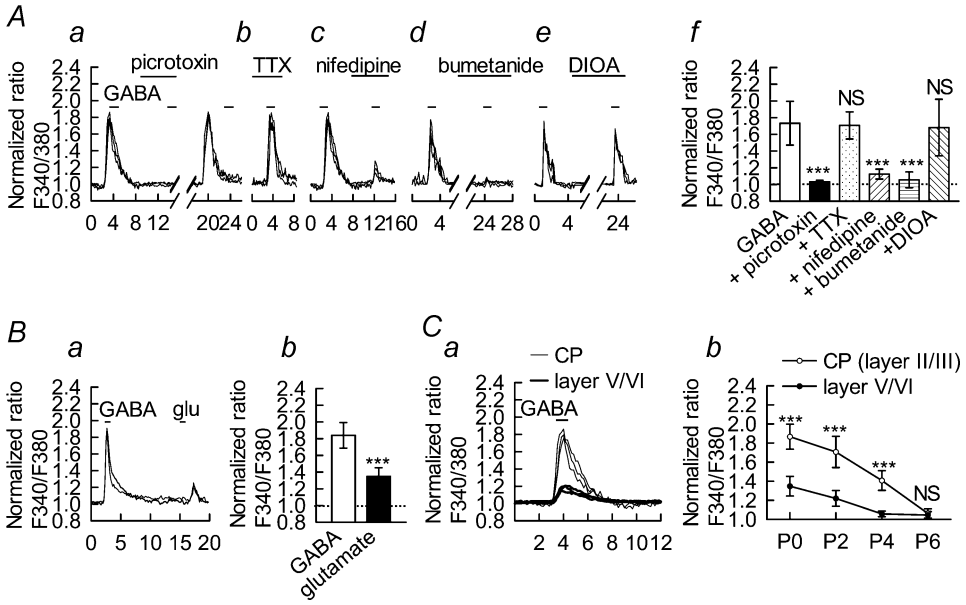

Figure 8. Changes in $[Ca^{2+}]_i$ response to GABA application in developing cortical neurones
A, CP neurones (P2) showed $[Ca^{2+}]_i$ elevations in response to GABA (10 μM). Picrotoxin (50 μM) reversibly abolished these responses (*a*). Even in the presence of TTX (3 μM), GABA still evoked equivalent $[Ca^{2+}]_i$ increases (*b*). However, nifedipine (100 μM) attenuated the GABA-induced response (*c*). After 20 min of bumetanide (20 μM) perfusion, the GABA-induced $[Ca^{2+}]_i$ elevations were completely abolished (*d*), whereas DIOA had no effect on such elevations (*e*). *f*, summary of effects of drugs on GABA-induced $[Ca^{2+}]_i$ elevations (***$P < 0.001$, ANOVA followed by Dunnett's test). *B*, in P1 CP neurones, the GABA (10 μM)-evoked $[Ca^{2+}]_i$ elevations were significantly ($P < 0.001$) greater than the glutamate (10 μM)-induced elevations. *C*, the GABA-induced Ca^{2+} transients were significantly larger in CP than in layer V/VI neurones at P2 (*a*). The difference gradually decreased as development proceeded, with no significant difference being observed between layer II/III and layer V/VI neurones at P6 (*b*) (***$P < 0.001$). Responses in three neighbouring cells in the same region of a single slice are shown in this figure. Error bars indicate S.D.

In contrast, during postnatal development KCC2 mRNA expression was initially low, then increased. Thus, a mechanism for Cl^- accumulation waned as a mechanism for Cl^- extrusion developed. When taken together with the results of pharmacological experiments, our data suggest that the higher $[Cl^-]_i$ in immature cells is maintained by the presence of an up-regulated NKCC1 and down-regulated KCC2.

Recently, it was proposed that KCC2, but not NKCC1, was involved in the developmental regulation of $[Cl^-]_i$ in immature auditory brainstem neurones (Balakrishnan *et al.* 2003). Although we cannot explain NKCC1 being non-functional in the auditory brainstem, the striking difference between brainstem and neocortex in the developmental course of NKCC1 suggests that other mechanisms, such as anion exchangers, might be operating instead of NKCC1 in the brainstem. It has also been reported that $[Cl^-]_i$ is strongly affected by membrane potential in rat retinal ON bipolar cells (Billups & Attwell, 2002). Thus, a passive Cl^- movement through membrane conductance may be involved in $[Cl^-]_i$ regulation. In any event, our results indicate that NKCC1 is an important homeostatic mechanism maintaining high $[Cl^-]_i$ in immature neocortical neurones, thus rendering GABA depolarizing.

Since these GABA-induced $[Ca^{2+}]_i$ elevations were attenuated by bumetanide, the high $[Cl^-]_i$ produced by the action of NKCC1 may enable GABA to depolarize CP neurones sufficiently to exceed the threshold for voltage-dependent Ca^{2+} channels.

In conclusion, our results suggest that NKCC1 may play a pivotal role in the generation of GABA-mediated Ca^{2+} transients in immature CP neurones, and hence in the migration, differentiation and synaptogenesis of these neurones (for review, see Ben-Ari, 2002; Owens & Kriegstein, 2002) while KCC2 promotes the later maturation of the GABAergic inhibitory system in pyramidal neurones. The factors that up-regulate NKCC1 expression in neuronal progenitors in the ventricular zone and down-regulate it soon after migration (Li *et al.* 2002; Shimizu-Okabe *et al.* 2002) remain to be identified.

References

Balakrishnan V, Becker M, Lohrke S, Nothwang HG, Guresir E & Friauf E (2003). Expression and function of chloride transporters during development of inhibitory neurotransmission in the auditory brainstem. *J Neurosci* **23**, 4134–4145.

Behar TN, Li YX, Tran HT, Ma W, Dunlap V, Scott C & Barker JL (1996). GABA stimulates chemotaxis and chemokinesis of embryonic cortical neurones via calcium-dependent mechanisms. *J Neurosci* **16**, 1808–1818.

Ben-Ari Y (2002). Excitatory actions of GABA during development: the nature of the nurture. *Nat Rev Neurosci* **3**, 728–739.

Ben-Ari Y, Cherubini E, Corradetti R & Gaiarsa JL (1989). Giant synaptic potentials in immature rat CA3 hippocampal neurones. *J Physiol* **416**, 303–325.

Billups D & Attwell D (2002). Control of intracellular chloride concentration and GABA response polarity in rat retinal ON bipolar cells. *J Physiol* **545**, 183–198.

Brooks-Kayal AR, Jin H, Price M & Dichter MA (1998). Developmental expression of $GABA_A$ receptor subunit mRNAs in individual hippocampal neurons in vitro and in vivo. *J Neurochem* **70**, 1017–1028.

Cherubini E, Rovira C, Gaiarsa JL, Corradetti R & Ben-Ari Y (1990). GABA mediated excitation in immature rat CA3 hippocampal neurons. *Int J Dev Neurosci* **8**, 481–490.

Clayton GH, Owens GC, Wolff JS & Smith RL (1998). Otogeny of cation-Cl^- cotransporter expression in rat neocortex. *Brain Res Dev Brain Res* **109**, 281–292.

Connor JA, Tseng HY & Hockberger PE (1987). Depolarization- and transmitter-induced changes in intracellular Ca^{2+} of rat cerebellar granule cells in explant cultures. *J Neurosci* **7**, 1384–1400.

Coull JA, Boudreau D, Bachand K, Prescott SA, Nault F, Sik A, De Koninck P & De Koninck Y (2003). Trans-synaptic shift in anion gradient in spinal lamina I neurons as a mechanism of neuropathic pain. *Nature* **424**, 938–942.

Dallwig R, Deitmer JW & Backus KH (1999). On the mechanism of GABA-induced currents in cultured rat cortical neurons. *Pflugers Arch* **437**, 289–297.

DeFazio RA, Keros S, Quick MW & Hablitz JJ (2000). Potassium-coupled chloride cotransport controls intracellular chloride in rat neocortical pyramidal neurons. *J Neurosci* **20**, 8069–8076.

Delpire E, Lu J, England R, Dull C & Thorne T (1999). Deafness and imbalance associated with inactivation of the secretory Na-K-2Cl co-transporter. *Nat Genet* **22**, 192–195.

Ebihara S, Shirato K, Harata N & Akaike N (1995). Gramicidin-perforated patch recording: GABA response in mammalian neurones with intact intracellular chloride. *J Physiol* **484**, 77–86.

Garay RP, Nazaret C, Hannaert PA & Cragoe EJ Jr (1988). Demonstration of a $[K^+,Cl^-]$-cotransport system in human red cells by its sensitivity to [(dihydroindenyl)oxy]alkanoic acids: regulation of cell swelling and distinction from the bumetanide-sensitive $[Na^+,K^+,Cl^-]$-cotransport system. *Mol Pharmacol* **33**, 696–701.

Gillen CM, Brill S, Payne JA & Forbush B III (1996). Molecular cloning and functional expression of the K-Cl cotransporter from rabbit, rat, and human. A new member of the cation-chloride cotransporter family. *J Biol Chem* **271**, 16237–16244.

Gillen CM & Forbush B III (1999). Functional interaction of the K-Cl cotransporter (KCC1) with the Na-K-Cl cotransporter in HEK-293 cells. *Am J Physiol* **276**, C328–C336.

Hicks SP & D'Amato CJ (1968). Cell migrations to the isocortex in the rat. *Anat Rec* **160**, 619–634.

Jarolimek W, Lewen A & Misgeld U (1999). A furosemide-sensitive K^+-Cl^- cotransporter counteracts intracellular Cl^- accumulation and depletion in cultured rat midbrain neurons. *J Neurosci* **19**, 4695–4704.

Kaila K, Pasternack M, Saarikoski J & Voipio J (1989). Influence of GABA-gated bicarbonate conductance on potential, current and intracellular chloride in crayfish muscle fibres. *J Physiol* **416**, 161–181.

Kaila K & Voipio J (1987). Postsynaptic fall in intracellular pH induced by GABA-activated bicarbonate conductance. *Nature* **330**, 163–165.

Kaila K, Voipio J, Paalasmaa P, Pasternack M & Deisz RA (1993). The role of bicarbonate in $GABA_A$ receptor-mediated IPSPs of rat neocortical neurones. *J Physiol* **464**, 273–289.

Kakazu Y, Uchida S, Nakagawa T, Akaike N & Nabekura J (2000). Reversibility and cation selectivity of the K^+-Cl^- cotransport in rat central neurons. *J Neurophysiol* **84**, 281–288.

Kelsch W, Hormuzdi S, Straube E, Lewen A, Monyer H & Misgeld U (2001). Insulin-like growth factor 1 and a cytosolic tyrosine kinase activate chloride outward transport during maturation of hippocampal neurons. *J Neurosci* **21**, 8339–8347.

Kilb W, Okabe A, Ikeda M, Shimizu-Okabe C, Yamada J, Fukuda A & Luhmann HJ (2002). Chloride regulation in Cajal-Retzius cells of the neonatal rat cerebral cortex. *Soc Neurosci Abstract* **28**, 431.3.

Leinekugel X, Tseeb V, Ben-Ari Y & Bregestovski P (1995). Synaptic $GABA_A$ activation induces Ca^{2+} rise in pyramidal cells and interneurons from rat neonatal hippocampal slices. *J Physiol* **487**, 319–329.

Li H, Tornberg J, Kaila K, Airaksinen MS & Rivera C (2002). Patterns of cation-chloride cotransporter expression during embryonic rodent CNS development. *Eur J Neurosci* **16**, 2358–2370.

LoTurco JJ, Owens DF, Heath MJ, Davis MB & Kriegstein AR (1995). GABA and glutamate depolarize cortical progenitor cells and inhibit DNA synthesis. *Neuron* **15**, 1287–1298.

Luhmann HJ & Prince DA (1991). Postnatal maturation of the GABAergic system in rat neocortex. *J Neurophysiol* **65**, 247–263.

Luhmann HJ, Schubert D, Kotter R & Staiger JF (1999). Cellular morphology and physiology of the perinatal rat cerebral cortex. *Dev Neurosci* **21**, 298–309.

Moore-Hoon ML & Turner RJ (1998). Molecular and topological characterization of the rat parotid Na^+-K^+-$2Cl^-$ cotransporter1. *Biochim Biophys Acta* **1373**, 261–269.

Nudel U, Zakut R, Shani M, Neuman S, Levy Z & Yaffe D (1983). The nucleotide sequence of the rat cytoplasmic beta-actin gene. *Nucl Acids Res* **11**, 1759–1771.

Owens DF, Boyce LH, Davis MB & Kriegstein AR (1996). Excitatory GABA responses in embryonic and neonatal cortical slices demonstrated by gramicidin perforated-patch recordings and calcium imaging. *J Neurosci* **16**, 6414–6423.

Owens DF & Kriegstein AR (2002). Is there more to GABA than synaptic inhibition? *Nat Rev Neurosci* **3**, 715–727.

Payne JA (1997). Functional characterization of the neuronal-specific K-Cl cotransporter: implications for $[K^+]_o$ regulation. *Am J Physiol* **273**, C1516–C1525.

Payne JA, Rivera C, Voipio J & Kaila K (2003). Cation-chloride co-transporters in neuronal communication, development and trauma. *Trends Neurosci* **26**, 199–206.

Plotkin MD, Snyder EY, Hebert SC & Delpire E (1997). Expression of the Na-K-2Cl cotransporter is developmentally regulated in postnatal rat brains: a possible mechanism underlying GABA's excitatory role in immature brain. *J Neurobiol* **33**, 781–795.

Rivera C, Voipio J, Payne JA, Ruusuvuori E, Lahtinen H, Lamsa K, Pirvola U, Saarma M & Kaila K (1999). The K^+/Cl^- co-transporter KCC2 renders GABA hyperpolarizing during neuronal maturation. *Nature* **397**, 251–255.

Shimizu-Okabe C, Yokokura M, Okabe A, Ikeda M, Sato K, Kilb W, Luhmann HJ & Fukuda A (2002). Layer-specific expression of Cl^- transporters and differential $[Cl^-]_i$ in newborn rat cortex. *Neuroreport* **13**, 2433–2437.

Staley KJ, Soldo BL & Proctor WR (1995). Ionic mechanisms of neuronal excitation by inhibitory $GABA_A$ receptors. *Science* **269**, 977–981.

Sun D & Murali SG (1999). Na^+-K^+-$2Cl^-$ cotransporter in immature cortical neurons: a role in intracellular Cl^- regulation. *J Neurophysiol* **81**, 1939–1948.

Sung KW, Kirby M, McDonald MP, Lovinger DM & Delpire E (2000). Abnormal $GABA_A$ receptor-mediated currents in dorsal root ganglion neurons isolated from Na-K-2Cl cotransporter null mice. *J Neurosci* **20**, 7531–7538.

Toyoda H, Ohno K, Yamada J, Ikeda M, Okabe A, Sato K, Hashimoto K & Fukuda A (2003). Induction of NMDA and $GABA_A$ receptor-mediated Ca^{2+} oscillations with KCC2 mRNA downregulation in injured facial motoneurons. *J Neurophysiol* **89**, 1353–1362.

Tyzio R, Ivanov A, Bernard C, Holmes GL, Ben Ari Y & Khazipov R (2003). Membrane potential of CA3 hippocampal pyramidal cells during postnatal development. *J Neurophysiol* **90**, 2964–2972.

Valverde F, Facal Valverde MV, Santacana M & Heredia M (1989). Development and differentiation of early generated cells of sublayer VIb in the somatosensory cortex of the rat: a correlated Golgi and autoradiographic study. *J Comp Neurol* **290**, 118–140.

Van Aubel RA, Peters JG, Masereeuw R, Van Os CH & Russel FG (2000). Multidrug resistance protein mrp2 mediates ATP-dependent transport of classic renal organic anion p-aminohippurate. *Am J Physiol Renal Physiol* **279**, F713–F717.

Yamada J, Okabe A, Toyoda H & Fukuda A (2002). Development of GABAergic responses and Cl^- homeostasis are regulated by differential expression of cation-Cl^- cotransporters: gramicidin-perforated patch-clamp and single cell multiplex RT-PCR study. *Soc Neurosci Abstract* **28**, 148.4.

Yuste R & Katz LC (1991). Control of postsynaptic Ca^{2+} influx in developing neocortex by excitatory and inhibitory neurotransmitters. *Neuron* **6**, 333–344.

Acknowledgements

We thank Dr K. Kaila for comments on an early version of this paper and Dr R. Timms for language-editing. This work was supported by Grants-in-Aid for Scientific Research on Priority Areas – Advanced Brain Science Project no. 13210065, 1401704, and 15016051 from the Ministry of Education, Culture, Sports and Science and Technology, Japan (A.F), by a JSPS-DFG Cooperative Research Grant (A.F), by Grant-in-Aid for Scientific Research no. 15590207 (J.Y) from the Japan Society for the Promotion of Science, and by DFG grants Lu 375/4-1 and 446-JAP-111/1/01 (H.J.L).